University of Huddersfield Repository

Tran, Van Tung and Yang, Bo-Suk

Machine fault diagnosis and condition prognosis using classification and regression trees and neuro-fuzzy inference systems

Original Citation

Tran, Van Tung and Yang, Bo-Suk (2010) Machine fault diagnosis and condition prognosis using classification and regression trees and neuro-fuzzy inference systems. Control and Cybernetics, 39 (1). pp. 25-54. ISSN 0324-8569

This version is available at http://eprints.hud.ac.uk/id/eprint/16579/

The University Repository is a digital collection of the research output of the University, available on Open Access. Copyright and Moral Rights for the items on this site are retained by the individual author and/or other copyright owners. Users may access full items free of charge; copies of full text items generally can be reproduced, displayed or performed and given to third parties in any format or medium for personal research or study, educational or not-for-profit purposes without prior permission or charge, provided:

- The authors, title and full bibliographic details is credited in any copy;
- A hyperlink and/or URL is included for the original metadata page; and
- The content is not changed in any way.

For more information, including our policy and submission procedure, please contact the Repository Team at: E.mailbox@hud.ac.uk.

http://eprints.hud.ac.uk/

Machine fault diagnosis and condition prognosis using classification and regression trees and neuro-fuzzy inference systems

Van Tung Tran, Bo-Suk Yang*

School of Mechanical Engineering, Pukyong National University, San 100, Yongdang-dong, Nam-gu, Busan 608-739, South Korea

Abstract

This paper presents an approach to machine fault diagnosis and condition prognosis based on classification and regression tress (CART) and neuro-fuzzy inference systems (ANFIS). In case of diagnosis, CART, which is one of the decision tree methods, is used as a feature selection tool to select pertinent features from data set and ANFIS is used as a classifier. The crisp rules obtained from CART are then converted to fuzzy if-then rules that are employed to identify the structure of ANFIS classifier. The hybrid of back-propagation and least squares algorithm are utilized to tune the parameters of the membership functions. The data sets obtained from vibration signals and current signals of the induction motors are used to evaluate the proposed algorithm. In case of prognosis, both of these models in association with direct prediction strategy for long-term prediction of time series techniques are utilized to forecast the future values of machine's operating condition. In this case, the number of available observations and the number of predicted steps are initially determined by using false nearest neighbor method and auto mutual information technique, respectively. These values are subsequently utilized as inputs for prediction models. The performance of the proposed prognosis system is then evaluated by using real trending data of a low methane compressor. A comparative study of the predicted results obtained from CART and ANFIS models is also carried out to appraise the prediction capability of these models. The results of the proposed methods in the two cases indicate that CART and ANFIS offers a potential for machine fault diagnosis as well as for condition prognosis.

Keywords: Fault diagnosis; Classification; Induction motors; Decision trees; Forecasts; Fuzzy systems.

1. Introduction

The fault progression process of mechanical systems usually consists of a series of degraded states due to component wear and fatigue during the operation process. Early detection of incipient faults and foretelling the future states of mechanical systems can minimize the costs of unnecessary maintenance, avoid unplanned breakdown and enable maintenance actions to be scheduled more effectively. Thence, the availability and reliability of machine will be increased. Consequently, machine fault diagnosis and machine condition prognosis have been the considerable subjects of researches in recent years.

1.1. Machine diagnosis of induction motors

Machine fault diagnosis is the ability to detect fault, isolate which component is failure, and decide on the potential impact of failed component on the health of the system. Due to the costs of implementing, only the critical machine components of which failures drastically affect the breakdown are frequently examined. In this study, induction motors are considered due to their indispensable roles in several industrial applications. The faults of induction motors may not only cause the interruption of product operation but also increase costs, decrease product quality and effect safety of operators. Consequently, fault diagnosis in induction motors has been the subject of considerable research in recent years.

The most common faults of induction motors are bearing failures, stator phase winding failures, broken rotor bar or cracked rotor end-rings and air-gap irregularities [1]. In order to detect/diagnose these faults, system identification and parameter estimation [2-6] as well as other techniques [7-10] have been proposed. These techniques required expensive equipment or accurate mathematical models which are challenging to describe the fault of motors. On the contrary, fuzzy logic and artificial neural networks (ANNs) can be used to provide inexpensive but effective fault detection mechanism alternatives [11]. ANNs are good at mapping non-linear numerical information between inputs and outputs. However, ANNs are not interpretable and understandable, i.e. they are incapable of explaining a particular decision to the user in a human-comprehensible form. Conversely, fuzzy logic has the ability of modeling human knowledge in a form of if-then rules using easily understandable linguistic term. In the case of machine fault diagnosis which involves high levels of uncertainty due to the complexity of machine systems and unexpected disturbance and noise in sensing [12], fuzzy logic can handle situations where the answer lies somewhere in-between. Some fuzzy logic based diagnosis approaches for induction motors have been proposed in [13-15]. Nevertheless, the if-then rules as well as the initial parameters of membership functions are normally prepared by an expert. Thus, fuzzy logic requires fine-turning in order to obtain acceptable rule base and optimize parameters for available data [15]. The individual problems from fuzzy logic or ANN alone can be solved by the integration of both methods and has been applied for motor fault diagnosis [11].

The adaptive neuro-fuzzy inference system (ANFIS) [16] is an integration of the ANNs adaptive capability and the fuzzy logic qualitative approach. It has been successfully applied for automated fault detection and diagnosis of induction machines [15, 17]. Recently, ANFIS and its combination with other methods were also employed as an enhanced tool for fault classification. Some examples of the combined algorithms are ANFIS with genetic algorithms [18] and ANFIS with wavelet transform [19] for bearing fault diagnosis. ANFIS has been also applied in classifying the faults of induction motor with variable driving speed [20].

Generally, the data obtained from measurements is high dimension and have a large amount of redundant features. If the data are directly inputted into the classifier, the performance will be significantly decreased. Feature extraction and selection have been utilized for reducing the dimension of data by selecting important features wherein feature extraction means and transforming the existing features into a lower dimensional space [21]. Nevertheless, each feature set contains many redundant or irrelevant features as well as salient features in feature space after the feature extraction has been done. Consequently, there is a need for feature selection tool to achieve good learning, classification accuracy, compact and easily understood knowledge-base, and a reduction in computational time [22].

In this study, CART [23] and ANFIS are utilized as feature selection tool and classifier for fault diagnosis of induction motors, respectively. This proposed system consists of two stages. First, the CART is performed to obtain the valuable features and identifies the structure of classifier in the next iterative step. Second, the ANFIS classifier is used to diagnose the faults of induction motors in which the parameters of membership functions are tuned throughout the learning process.

1.2. Machine condition prognosis

Prognosis is the ability to predict accurately the future health states and failure modes based on current health assessment and historical trends [24]. There are two main functions of machine prognosis: failure prediction and remaining useful life (RUL) estimation. Failure prediction, which is addressed in this paper, allows pending failures to be identified early before they come to more serious failures that result machine breakdown and repair costs. RUL is the time left before a particular fault will occur or the part needs to be replaced. The techniques related to prognosis can be broadly classified as experience-based, model-based, and data-driven based techniques.

Experience-based prognostic approaches require the component failure history data or operational usage profile data. They involve in collecting statistical information from a large number of component samples to indicate the survival duration of a component before a failure occurs and use these statistical parameters to predict the RUL of individual components. Generally, they are the least complex forms of prognostic techniques and their accuracy is not high because they base solely on the analysis of the past experience.

Model-based prognostic approaches are applicable to where the accurate mathematical models can be constructed based on the physical fundamentals of a system. These approaches use residuals as features, which are the outcomes of consistency checks between the sensed measurements of system and the outputs of a mathematical model [25]. Some of the published researches using these approaches can be found in references [25-30]. However, even though the accuracy of these techniques is reasonably high, they are only suitable for specific components and each component requires a specific mathematical model. Changes in structural dynamics and operating conditions can affect the mathematical model which is impossible to mimic all real-life situations.

Data-driven prognosis techniques utilize and require a large amount of historical failure data to build a prognostic model that learns the system behavior. Among these techniques, artificial intelligence is regularly used because of its flexibility in generating appropriate models. Reference [31] gives a survey on artificial intelligent techniques used in prognosis. Other outstanding data-driven prognosis techniques can be found in references [32-35]. In comparison with other prognosis techniques, data-driven prognosis techniques are the most promising and effective techniques in machine condition prognosis. They frequently use vibration signals for temporal pattern identifications since it is relatively easy to measure and record machine vibration data. Accordingly, data-driven prognosis technique with vibration-based measurement are developed and used for machine condition prognosis in this study.

In addition, the more future states are predicted precisely, the more effective the maintenance activities become. For that reason, long-term prediction methodology is considered in machine condition prognosis significantly. Nevertheless, forecasting the future with long-term prediction strategy is still a difficult and challenging task in time series prediction domain due to the growing uncertainties arising from unrelated sources, such as, accumulation errors and insufficient information [36]. The techniques of long-term prediction methodology will be described in the next section.

In long-term prediction, embedding dimension (ED), time delay (TM), and selection prediction model are essential to be considered. ED and TM are used to reconstruct the space state of machine's condition time series and establish the fundamental parameters of prediction model. ED is the number of initial observations that should be used as the inputs for prediction model. This value can be determined by using the false nearest neighbor method (FNN) [37] or the Cao's method [38]. Of the two suggested methods, the FNN method is commonly used.

Time delay is the number of steps that can be predicted by the prediction model to obtain the optimum performance. It can be calculated by using some of the published methods such as auto-correlation [39], average displacement [40], and auto-mutual information (AMI) [41]. In this study, AMI is chosen to estimate the time delay. After determining the embedding dimension and time delay, CART and ANFIS are utilized as the prediction model for the purposes of comparing the forecasting ability for long-term prediction in the machine condition.

2. Background knowledge and proposed systems

2.1 Background knowledge

2.1.1 Long-term prediction strategies

In time series domain, prediction techniques consist of short-term prediction (one-step ahead prediction) and long-term prediction (multi-step ahead prediction). Unlike the short-term prediction, the long-term prediction is typically faced with growing uncertainties arising from various sources. According to Sorjamaa et al. [42], there are three strategies mainly used in long-term prediction. They are recursive, direct, and DirRec strategies that could be frequently used for creating prediction model. The detailed information of these strategies could be found in reference [43]

2.1.2. Time delay (TM) estimation

There are several methods published in literature could be used to choose the TM. However, most of them are based on empirical concepts and it is not easy to identify which of the methods is suitable for a particular task. In this paper, TM is dealt with auto mutual information (AMI) method. The mutual information (MI) can be used to evaluate the dependence among random variables. The MI between two variables, let X and Y be the amount of information obtained from X in the presence of Y and vice versa. In time series prediction problem, if Y is the output and X is a subset of the input variables, the MI between X and Y is one criterion for measuring the dependence between inputs and output. Thus, the inputs subset X, which gives maximum MI, is chosen to predict the output Y. The MI between two measurements taken from a single time series $x(t)$ separated by time τ is called the AMI. The detailed theory of AMI was presented in references [41-42, 44]. AMI estimates the degree to which the time series $x(t+\tau)$ on average can be predicted from a given time series $x(t)$, i.e. the mean predictability of future values in the time series from the past values.

The AMI between $x(t)$ and $x(t+\tau)$ is:

$$I_{XX_\tau} = \sum_{x(t),x(t+\tau)} P_{XX_\tau}(x(t), x(t+\tau)) \ln\left(\frac{P_{XX_\tau}(x(t), x(t+\tau))}{P_X(x(t))P_{X_\tau}(x(t+\tau))}\right) \tag{1}$$

where $P_X(x(t))$ is the normalized histogram of the distribution of values observed for $x(t)$ and $P_{XX_\tau}(x(t), x(t+\tau))$ is the joint probability density for the measurements of $x(t)$ and $x(t+\tau)$.

The decreasing rate of the AMI with increasing time delay is a normalized measure of the time series' complexity. The first local minimum of the AMI of time series has been used to determine the optimal TM.

2.1.3. Determining the embedding dimension (ED)

After calculating the TM, ED is the next parameter to be determined. FNN method is employed in this study and will be briefly explained. Assuming that a time-series of $x_1, x_2, ..., x_N$ and vector $y_i(d)$, which is given in equation (2), in a delay coordinate embedding of the time series with time delay τ and embedding dimension d are given.

$$y_i(d) = [x_i, x_{i+\tau}, ..., x_{i+(d-1)\tau}], \quad i = 1, 2, ..., N-(d-1)\tau \tag{2}$$

The observations x_i are projections of the system's trajectory in the multivariate state space onto 1-dimensional axis. The FNN method is based on the concept that in the passage from dimension d to dimension d+1, where one can differentiate between points which are 'true" or "false" neighbor on the orbit. For instance in Figure 1, points A, B, C and D belong to a curve. In 1-dimension, points A and D appear to be nearest neighbor. However, point D is no longer nearest neighbor of point A in 2-dimension. In the same way, points A and C are nearest neighbor in 2-dimension but they are no longer neighbors when viewed in 3-dimension. In this case, points A, D, C are examples of "false" neighbors while points A and B are "true" neighbors.

Fig. 1 An example of false nearest neighbors

The criteria for identification of false nearest neighbors can be explained as follows: denote $y_i^r(d)$ as the nearest neighbor of $y_i(d)$ in a d dimensional embedding space. According to [19], the nearest neighbor is determined by finding the vector which minimizes the Euclidean distance:

$$R_d = \left\| y_i(d) - y_i^r(d) \right\| \tag{3}$$

Considering each of these vectors under a d+1 dimensional embedding:

$$y_i(d+1) = [x_i, x_{i+\tau}, x_{i+2\tau}, ..., x_{i+d\tau}], \quad i = 1, 2, ..., N-d\tau \tag{4}$$

$$y_i^r(d+1) = [x_i^r, x_{i+\tau}^r, x_{i+2\tau}^r, ..., x_{i+d\tau}^r], \quad i = 1, 2, ..., N-d\tau \tag{5}$$

The vectors are separated by the Euclidean distance:

$$R_{d+1} = \left\| y_i(d+1) - y_i^r(d+1) \right\| \tag{6}$$

The first criterion of FNN which identifies a false nearest neighbor is:

$$\sqrt{\frac{R_{d+1}^2 - R_d^2}{R_d^2}} = \frac{\left| x_{i+d\tau} - x_{i+d\tau}^r \right|}{R_d} > R_{tol} \tag{7}$$

where R_{tol} is a tolerance level.

The second criterion is:

$$\frac{R_{d+1}}{R_A} > A_{tol} \tag{8}$$

where R_A is a measure of the size of the attractor and A_{tol} is a threshold that can be chosen in practice. If both equations (7) and (8) are satisfied, then $y_i^r(d)$ is a false nearest neighbor of $y_i(d)$. Once the total number of FNN is calculated, the percentage of FNN is measured. An appropriate ED is the value where the percentage of FNN falls to zero.

2.1.4. Classification and regression trees (CART) and adaptive neuro-fuzzy inference system (ANFIS) model

CART algorithm has been extensively developed by Breiman et al. [23] for classification or regression purpose depending on the response variable which is either categorical or numerical. In case of classification, CART induces strictly binary trees through a process of binary recursively partitioning of feature space of a data set [45]. Similarly, in case of regression, a binary tree is constructed with the repeated splits of the subsets into two descendant subsets according to independent variables. The goal is to produce subsets of the data which are as homogeneous as possible with respect to the response variables. Either classification tree or regression tree consists of the following two processes: tree growing and tree pruning. The detailed theory of these processes can be found in [23, 45, 47].

ANFIS is a fuzzy Sugeno model put in the framework of adaptive systems to facilitate learning and adaptation [16]. Such framework makes the ANFIS modeling more systematic and less dependent on expert knowledge. In order to present ANFIS architecture, two fuzzy if-then rules based on a first-order Sugeno model are considered:

Rule 1: If (x is A_1) and (y is B_1) then $f_1 = p_1 x + q_1 y + r_1$.

Rule 2: If (x is A_2) and (y is B_2) then $f_2 = p_2 x + q_2 y + r_2$.

where x and y are the inputs, f_i are the outputs within the fuzzy region specified by the fuzzy rule, A_i and B_i are the fuzzy sets, $\{p_i, q_i, r_i\}$ is a set of design parameters that are determined during the learning process. The ANFIS architecture to implement these rules and the learning algorithm to tune all the modifiable parameters could be referred to [43, 45-46].

2.2. Proposed systems

2.2.1. Machine fault diagnosis

In this study, the vibration signals and current signals are utilized for detecting the faults of induction motors. The proposed system consists of four procedures as in Fig. 2: data acquisition, feature calculation, feature reduction, and fault classification. The summary role of each procedure is described as follow:

Data acquisition: this procedure is used to attain the vibration signals and current signals. Furthermore, data processing is also carried out.

Feature calculation: the most significant features are calculated by using statistical feature parameters from time domain and frequency domain.

Feature selection: the CART algorithm is used to select the salient features from the whole feature set.

Fault classification: The data obtained from feature reduction procedure is split into two data sets: training and testing data. Training data is employed to build the model whilst testing data is for validating the model. The results indicate the accuracy of classification

Fig. 2 Proposed system for fault diagnosis

2.2.2. Machine condition prognosis

The proposed system for prognosis of machine condition comprises four procedures sequentially as shown in Fig. 3, namely, data acquisition, data splitting, training-validating model, and predicting. The role of each procedure is explained as follows:

Data acquisition: this procedure is used to obtain the vibration data from machine condition. It covers a range of data from normal operation to obvious faults of the machine.

Data splitting: the trending data attained from previous procedure is split into two parts: training set and testing set. Different data is used for different purposes in the prognosis system. Training set is used for creating the prediction models whilst testing set is utilized to test the trained models.

Training-validating: this procedure includes the following sub-procedures: estimating the TM and determining the ED based on AMI and FNN method, respectively; creating the prediction models and validating those models. Validating the prediction models are used for measuring their performance capability.

Predicting: long-term direct prediction method is used to forecast the future values of machine condition. The predicted results are measured by the error between predicted values and actual values in the testing set. Updating models are also carried out in this procedure for the next prediction process.

Fig. 3 Proposed system for machine condition prognosis

3. Experiments

3.1. Machine fault diagnosis

To validate CART-ANFIS model, experiment was carried out using a test-rig which consists of a motor, pulleys, belt, shaft and fan with changeable blade pitch angle that represents the load. The load can be changed by adjusting blade pitch angle or the number of blades. Six induction motors of 0.5 kW, 60 Hz, 4-pole were used to create data. One of the motors with good condition (healthy) is used for comparison with faulty motors. The others are faulty motors, with rotor unbalance, broken rotor bar, phase unbalance, bearing outer race fault, bowed rotor, and adjustable eccentricity motor, as shown in Fig. 4. The conditions of faulty motors are described in Table 1.

Fig. 4 Faults on the induction motors

Table 1 The description of faulty motors

For acquiring data from test rig, three AC current probes and three accelerometers were used to measure the stator current of the three-phase power supply and vibration signal in the horizontal, vertical, axial directions for evaluating the fault diagnosis system, respectively. The maximum frequency of the signal was 3 kHz, with 16,384 sampled data and giving a measured time of 2.133 s.

3.2 Machine condition prognosis

The proposed method is applied to a real system to predict the trending data of a low methane compressor which is important equipment in petrochemical plant. This compressor is driven by a 440 kW motor, 6600 volt, 2 poles and operating at a speed of 3565 rpm. Other information of the system is summarized in Table 2.

Table 2 Information of the system

The condition monitoring system of this compressor consists of two types: off-line and on-line. In the off-line system, the vibration sensors were installed along axial, vertical, and horizontal directions at the locations of drive-end motor, non drive-end motor, male rotor compressor and suction part of compressor. In the on-line system, acceleration sensors were located at the same places as in the off-line system but only in the horizontal direction.

The trending data were recorded from August 2005 to November 2005 which included peak acceleration and envelope acceleration data. The average recording duration was 6 hours during the data acquisition process. Each data record consisted of approximately 1200 data points as shown in Figs. 5 and 6, and contained information of machine history with respect to time sequence (vibration amplitude). Consequently, it can be classified as time-series data.

Fig. 5 The entire peak acceleration data of low methane compressor

Fig. 6 The entire envelope acceleration data of low methane compressor

These figures show that the machine was in normal condition during the first 300 points of the time sequence. After that time, the condition of the machine suddenly changed, indicating that possible faults were occurring in the machine. By disassembling and inspecting, these faults were identified as the damage of main bearings of the compressor (notation Thrust: 7321 BDB) due to insufficient lubrication. Consequently, the surfaces of these bearings were overheated and delaminated [47]. With the aim of forecasting the change of machine condition, the first 300 points will be used to train the system.

4. Results and discussions

4.1. Machine fault diagnosis

4.1.1. Feature calculation

In this paper, the feature calculation using statistical feature parameters from time domain and frequency domain was used. Sixty-three (63) (21 parameters × 3 signals) features in total are calculated from 10 feature parameters of time domain. These parameters are mean, RMS, shape factor, skewness, kurtosis, crest factor, entropy error, entropy estimation and histogram of upper and lower limits. And three parameters from frequency domain (RMS frequency, frequency center and root variance frequency) using the three direction vibration signals and three-phase current signals. The total number of feature parameters is shown in Table 3. The data sets of the features have 270 samples. In each operating condition, 20 samples are employed for training process and 10 samples for testing. The detailed descriptions of those data sets are shown in Table 4.

Table 3 Feature parameters

Table 4 Descriptions of data sets

4.1.2. Feature selection and classification

The final trees obtained from the feature sets corresponding to the vibration signals and current signals are depicted in Figs. 7 and 8, respectively. Obviously, the feature appearing in root node of the trees is the most important one. The other features in remaining nodes appear in descending order of importance. It is to be emphasized which only features that contribute to the classification appear in the decision tree and the others do not. Features, which have less discriminating capability, can be consciously discarded by deciding on the threshold. From that, a number of features are strikingly diminished and only 4 features (x_2, x_5, x_{15} and x_{23}) of vibration signals and 7 features (x_2, x_5, x_6, x_8, x_{11}, x_{15} and x_{19}) of current signals are remained. The reduction of features will decrease the burden of computation for ANFIS classifier in the next step. Furthermore, these trees are also used to identify the structure of ANFIS classifier. This structure includes fuzzy rule set which has been fuzzyfied from the crisp set of tree and membership functions which bell-shaped functions are chosen in this system.

Fig. 7 Tree of features obtained from vibration signals
Fig. 8 Tree of features obtained from current signals

The system parameters and the chosen membership functions are automatically adjusted during the learning process. The convergence of the root mean squared (RMS) error is utilized to evaluate the learning process. If the decreasing rate of the RMS error as well as the performance is not significant, the learning process can be terminated. In this study, after 800 training epochs, the RMS error decreased to 0.087 and reached the convergent stage. This means the learning process can be terminated.

The classification results are calculated using a ten-fold cross-validation evaluation where the data set to be evaluated is randomly partitioned so that 180 samples are used for training and 90 samples are used for testing. The process is iterated with different random partitions and the results are averaged. The CART-ANFIS achieved 100% classification accuracy without any misclassification out of 180 samples of training data for vibration and current signals. After training, the CART-ANFIS was tested against the testing data. The confusion matrix showing the classification results of the CART-ANFIS created with 800 epochs of training cycle is given in Table 5. In confusion matrix, each cell contains the number of samples that was correctly classified corresponding to actual network outputs and desired outputs of vibration signals and current signals. For example, the number is shown as 10/7 in the first cell (the first column and the first row of confusion matrix) means that there were 10 outputs were belonged to class C1 and 7 outputs were belonged to class C1 for vibration signals and current signals, respectively. It is similar to the other cells in the diagonal of confusion matrix. The other cells that were not in the diagonal of confusion matrix indicate the misclassifications. For example, the cell being in the first column and the third row has the value as 0/1 shows that all subjects were correctly classified for vibration signals and one subject should have belonged to class C1 was classified as subjects of class C3.

The total classification accuracy for the test data was found as 91.11% with 8 misclassification out of 90 test samples for the vibration signal, while 76.67% with 21 misclassification out for the current signal.

The test performance of the classifier can be determined by the computation of statistical parameters such as sensitivity, specificity and total classification accuracy defined by:

Sensitivity: number of true positive decisions/ sum of number of true positive cases and number of false negative cases.

Specificity: number of true negative decisions/sum of number of true negative cases and number of false positive cases.

Total classification accuracy: number of correct decisions/total number of cases.

The values of statistical parameters are given in Table 6. The CART-ANFIS model classified C1 to C9 subject in form of a/b which implies the accuracy of classification corresponding to vibration signals and current signals as follows: 100/70, 100/80, 70/90, 90/80, 80/70, 100/70, 90/70, 100/80 and 90/80% for vibration and current signals, respectively. Those values are obtained from the cells that are in the diagonal of confusion matrix. All of the data sets were classified with the accuracy of 91.11%/76.67% (total classification accuracy).

Table 5 The confusion matrix for CART-ANFIS of 800 epochs

Table 6 The value of statistical parameters

4.2. Machine condition prognosis

Before being used to generate the prediction models, TM is initially calculated according to the method mentioned in section 2.1.2. Theoretically, the optimal time delay is the value at which the AMI obtains the first local minimum. From Fig. 9, the optimal TM of peak acceleration training data is found as 7. Similarly, 5 is the optimal TM value of envelope acceleration training data.

Fig. 9 Time delay estimation

Using FNN method described in section 2.1.3, the optimal TM is subsequently utilized to determine the embedding dimension d. It is noted that the tolerance level R_{tol} and threshold A_{tol} must be initially chosen. In this study, R_{tol} = 15 and A_{tol} = 2 are used according to the results from [37]. The relationship between the false nearest neighbor percentage and the embedding dimension for both peak acceleration data and envelope data is shown in Fig. 10. From the figure, the embedding dimension d is chosen as 4 for both data sets where the false nearest neighbor percentage reaches to 0.

Fig. 10 The relationship between FNN percentage and embedding dimension

Subsequent to determining the TM and ED, the process of generating the prediction models is carried out. Based on those values, the training data are created in which the number of observations is equal to ED and the number of predicted steps is equal to TM. Using this training data, the CART model and the ANFIS model are established. In case of the CART model, the number of response values for each terminal node in tree growing process is 5 and 10 cross-validations are decided for selecting the best tree in tree pruning. Furthermore, in order to evaluate the predicting performance, the root-mean square error (RMSE) is utilized as following

$$RMSE = \sqrt{\frac{\sum_{i=1}^{N}(y_i - \hat{y}_i)^2}{N}} \tag{9}$$

where N, y_i, $\hat{y}_i$ represent the total number of data points, the actual value, and predicted value of prediction model in the training data or testing data, respectively.

Figs. 11(a) and 12(a) perform the training and validating results of the CART models for peak acceleration and envelope acceleration data, respectively. The actual values and predicted values are almost identical with very small RMSE values ranging from 0.002217 to 1.3314×10^{-5}. It indicates that the learning capability of CART model is extremely good. Similarly, the ANFIS models are also created for both training set of peak acceleration and envelope acceleration. There are four inputs for each ANFIS model due to the embedding dimension value. For each input, a bell shape is chosen for each membership function (MF) and the number of MFs is 2. It means that the region value of each input is divided into two, namely, small and large. In order to evaluate the learning process, the convergence of RMSE is also utilized. In this study, after executing 100 epochs, all RMSEs of the outputs reach the convergent stage for both the peak acceleration data and envelope acceleration data as shown in Fig. 13. Alternatively, the parameters of MFs are automatically adjusted through the learning in order that the outputs of ANFIS model match the actual values in training data. The changes of MF shapes are depicted in Fig. 14. The training and validating results of ANFIS models for both the peak acceleration data and envelope acceleration data are respectively shown in Figs. 11(b) and 12(b). From these figures, the RMSE values are sequentially 0.00876 and 0.08886. These values are slightly higher than those of the CART models. The reason could be that the number of MFs is improperly chosen. For higher accuracy of RMSEs, the MFs can be increased. Nevertheless, this will also increase the computational complexity and take too much training time.

Fig. 11 Training and validating results of peak acceleration data. (a) CART, (b) ANFIS

Fig. 12 Training and validating results of envelope acceleration data. (a) CART, (b) ANFIS.

Fig. 13 RMSE convergent curve. (a) Peak acceleration, (b) Envelope acceleration.

Fig. 14 The changes of MFs after learning. (a) Peak acceleration, (b) Envelope acceleration.

Figs. 15 and 16 show the predicted results of the CART models and the ANFIS models for peak acceleration and envelope acceleration data. The RMSE values of the CART model and the ANFIS model for those data are summarized in Table 7. Although, the RMSEs of ANFIS models are slightly higher values than those of CART models in both cases of peak acceleration and envelope acceleration data, the predicted results of ANFIS models can keep track with the changes of the operating condition of machine more precisely. This is of crucial importance in industrial application for estimating the time-to-failure of equipments. As mentioned above, the predicted results of ANFIS models can be improved by adjusting the parameters of ANFIS. However, these changes should take into consideration the increase of computational complexity and time-consumption of the training process which may lead to unrealistic application in real life.

Fig. 15 Predicted results of peak acceleration data. (a) CART, (b) ANFIS.

Fig. 17 Predicted results of envelope acceleration data. (a) CART, (b) ANFIS.

Table 7 The RMSEs of CART and ANFIS

5. Conclusion

Machine fault diagnosis and condition prognosis are extremely essential in mechanical systems for detecting the faults and foretelling the degradation of operating conditions. In this study, an approach to machine fault diagnosis and condition prognosis based on CART and ANFIS has been investigated. In case of diagnosis, a combined CART and ANFIS have been presented to perform fault diagnosis of induction motors. The classification results and statistical measures were used for evaluating the CART-ANFIS model. The total classification accuracy was 91.11% and 76.67% for vibration and current signals, respectively. In case of prognosis, long-term direct prediction for the operating conditions of machine based on data-driven approach has been examined. The CART models and ANFIS models are validated by its ability to predict future state conditions of a low methane compressor using the peak acceleration and envelope acceleration data. The predicted results of CART models are slightly better than those of ANFIS. Nonetheless, they are incapable of tracking the change of machines' operating conditions with high accuracy as compared to ANFIS models. The tracking-change capability of operating conditions is of crucial importance in estimating the RUL of industrial equipments. The results confirm that the proposed systems in both cases offer a potential for machine fault diagnosis and condition prognosis.

References

[1] G.G. Acosta, C.J. Verucchi, E.R. Gelso, A current monitoring system for diagnosis electrical failures in induction motors, Mechanical Systems and Signal Processing 20 (2006) 953-965.

[2] A.K. Sood, A.A. Fahs, N.A. Henein, Engine fault analysis – part I: statistical methods, IEEE Transactions on Industrial Electronics 32 (1985) 294-300.

[3] A.K. Sood, A.A. Fahs, N.A. Henein, Engine fault analysis – part I: Parameter estimation approach, IEEE Transactions on Industrial Electronics 32 (1985) 301-307

[4] R. Isermann, Process fault detection based on modeling and estimation methods – a survey, Automatica 20 (1984) 387-404

[5] R. Isermann, B. Freyermuth, Process fault diagnosis based on process model knowledge – part I, Journal of Dynamic Systems, Measurement, and Control 113 (1991) 620-626

[6] K.R. Cho, J.H. Lang, S. Umans, Detection of broken rotor bars using state and parameter estimation, IEEE Transactions on Industry Applications 28 (1992) 702-713

[7] B.S. Yang, K.J. Kim, Application of Dampster-Shafer theory in fault diagnosis of induction motors using vibration and current signals, Mechanical Systems and Signal Processing 20 (2006) 403-420.

[8] B.S. Yang, S.K. Jeong, Y.M. Oh, A.C.C. Tan, Case-based reasoning with Petri nets for induction motors fault diagnosis, Expert Systems with Applications 27 (2) (2004) 301-311.

[9] R. Casimir, E. Boutleux, G. Clerc, A. Yahoui, The use of feature selection and nearest neighbors rule for faults diagnosis in induction motors, Engineering Applications of Artificial Intelligence 19 (2006) 169-177.

[10] A. Widodo, B.S Yang, T. Han, Combination of independent component analysis and support vector machines for intelligent faults diagnosis of induction motors, Expert Systems with Applications 32 (2) (2007) 299-312.

[11] P. Goode, M.Y. Chow, Using a neural/fuzzy to extract knowledge of incipient fault in induction motor: part 1- methodology, IEEE Trans. Industrial Electronics 42 (2) (1995) 131-138.

[12] Y. Chen, A fuzzy decision system for fault classification under high levels of uncertainty, Journal of Dynamic Systems, Measurement, and Control 117 (1995) 108-115

[13] B. Satish, N.D.R. Samar, A fuzzy approach for diagnosis and prognosis of bearing faults in induction motors, IEEE Power Engineering Society General Meeting 3 (2005) 2291-2294.

[14] M.E.H. Benbouzid, H. Nejjari, A simple fuzzy logic approach for induction motors stator

condition monitoring, Proceedings of the IEEE IEMDC2001, 2001, pp. 634-639.
[15] M. Shukri, M. Khalid, R. Yusuf, M. Shafawi, Induction machine diagnostic using adaptive neuron fuzzy inference system, M. Gh. Negoita et al. (Eds.), KES2004 (2004) 380-387.

[16] J.S.R. Jang, ANFIS: adaptive-network-based fuzzy inference system, IEEE Trans. System, Man and Cybernetics 23 (3) (1993) 665-685.
[17] S. Altug, M.Y. Chow, H.J. Trussell, Fuzzy inference systems implemented on neural architectures for motor fault detection and diagnosis, IEEE Trans. Industrial Electronics 46 (6) (1999) 1069-1079.
[18] Y. Lei, Z. He, Y. Zi, Q. Hu, Fault diagnosis of rotating machinery based on multiple ANFIS combination with GAs, Mechanical Systems and Signal Processing, in press.
[19] X. Lou, K.A. Loparo, Bearing fault diagnosis based on wavelet transform and fuzzy inference, Mechanical Systems and Signal Processing 18 (2004) 1077-1095.
[20] Z. Ye, A. Sadeghian, B. Wu, Mechanical fault diagnosis for induction motor with variable speed drives using adaptive neuro-fuzzy inference system, Electric Power Systems Research 76 (2006) 742-752.
[21] B.S. Yang, T. Han, Z.J. Yin, Fault diagnosis system of induction motors using feature extraction, feature selection and classification algorithm, JSME International Journal (C) 49 (3) (2006) 734-741.
[22] R. Kumar, V.K Jayaraman, R.D. Kulkarni, An SVM classifier incorporating simultaneous noise reduction and feature selection: illustrative case examples, Pattern Recognition 38 (2005) 41-49.
[23] L. Breiman, J.H. Friedman, R.A. Olshen, C.J. Stone, Classification and regression trees, Chapman & Hall Press, 1984.
[24] C.S. Byington, M. Watson, M.J Roemer, T.R. Galic, J.J. McGroarty, (2003). Prognostic enhancements to gas turbine diagnostic systems, Proceeding of IEEE Aerospace Conference 7 (2003) 3247-3255.
[25] F. Tu, S. Ghoshal, J. Luo, G. Biswas, S. Mahadevan, L. Jaw, K. Navarra, PHM integration with maintenance and inventory management systems, IEEE Aerospace Conference Digest, Motana, (2004) 1-12.
[26] M. Abbas, A.A. Ferri, M.E. Orchard, G.J. Vachtsevanos, An intelligent diagnostic/ prognostic framework for automotive electrical systems, Proceedings of the 2007 IEEE Intelligent Vehicles Symposium, Instanbul, (2007) 352-357.
[27] Y. Li, S. Billington, C. Zhang, T. Kurfess, S. Danyluk, S. Liang, Adaptive prognostics for rolling element bearing condition, Mechanical Systems and Signal Processing 13 (1) (1999) 103-113.
[28] Y. Li, T.R. Kurfess, S.Y. & Liang, Stochastic prognostics for rolling element bearings, Mechanical Systems and Signal Processing 14 (5) (2000) 747-762.
[29] M. Watson, C. Byington, D. Edwards, S. Amin, Dynamic modeling and wear-based remaining useful life prediction of high power clutch systems, Tribology Transactions 48 (2) (2005) 208-217.
[30] M. Luo, D. Wang, M. Pham, C.B. Low, J.B. Zhang, D.H. Zhang, Y.Z. Zhao, Model-based fault diagnosis/prognosis for wheeled mobile robots: a review. Proceedings of the 31st Annual Conference of IEEE Industrial Electronics Society, New York, (2005) 2267-2272.
[31] M. Schwabacher, K. Goebel, A survey of artificial intelligence for prognostics, Proceedings of AAAI Fall Symposium on Artificial Intelligence for Prognostics, 9-11 Nov., 2007.
[32] G. Vachtsevanos, P. Wang, Fault prognosis using dynamic wavelet neural networks, Proceedings of IEEE Systems Readiness Technology Conference (2001) 857-870.
[33] R. Huang, L. Xi, X. Li, C.R. Liu, H. Qiu, J. Lee, Residual life prediction for ball bearings based on self-organizing map and back propagation neural network methods, Mechanical Systems and Signal Processing 21 (2007) 193-207.

[34] W.Q. Wang, M.F. Golnaraghi, F. Ismail, Prognosis of machine health condition using neuro-fuzzy system, Mechanical System and Signal Processing 18 (2004) 813-831.
[35] E.R. Brown, N.N. McCollom, E. Moore, A. Hess, Prognostics and health management – a data-driven approach to supporting the F-35 Lightning II, Proceedings of IEEE Aerospace Conference, (2007) 1-12.
[36] Y. Ji, J. Hao, N. Reyhani, A. Lendasse, Direct and recursive prediction of time series using mutual information selection, Lecture Notes in Computer Science 3512 (2005) 1010-1017.
[37] M.B. Kennel, R. Brown, H.D.I. Abarbanel, Determining embedding dimension for phase-space reconstruction using a geometrical construction, Physical Review A 45 (1992) 3403-3411.
[38] L. Cao, Practical method for determining the minimum embedding dimension of a scalar time series, Physica D 110 (1997) 43-50.
[39] D.S. Broomhead, Extracting qualitative dynamics from experimental data, Physica D 20 (1986) 217-236.
[40] M.T. Rosenstein, J.J. Collins, C.J.D. Luca, Reconstruction expansion as a geometry-based framework for choosing proper delay time, Physica D 73 (1994) 82-89.
[41] A.M. Fraser, H.L. Swinney, Independent coordinates for strange attractors from mutual information, Phys. Rev. A 33 (1986) 1134-1140.
[42] A. Sorjamaa, A. Lendasse, Time series prediction as a problem of missing values: application to ESTSP and NN3 competition benchmarks, Proceedings of European Symposium on Time Series Prediction, (2007) 165-174.
[43] V.T. Tran, B.S. Yang, A.C.C. Tan, Multi-step ahead direct prediction for the machine condition prognosis using regression trees and neuro-fuzzy systems, Expert Systems with Applications 36 (2009) 9378-9387.
[44] A. Sorjamaa, J. Hao, N. Reyhani, Y. Ji, A. Lendasse, Methodology for long-term prediction of time series, Neurocomputing 70 (2007) 2861-2869.
[45] J.S.R. Jang, C.T. Sun, E. Mizutani, Neuro-fuzzy and soft computing: a computational approach to learning and machine intelligent, Prentice Hall, 1996.
[46] E. Ikonen, K. Najim, Fuzzy neural networks and application to the FBC process, Proceeding of Control Theory Application 143 (1996) 259-269.
[47] V.T. Tran, B.S. Yang, M.S. Oh, A.C.C. Tan, Machine condition prognosis based on regression trees and one-step-ahead prediction, Mechanical Systems and Signal Processing, 22 (2008) 1179-1193.

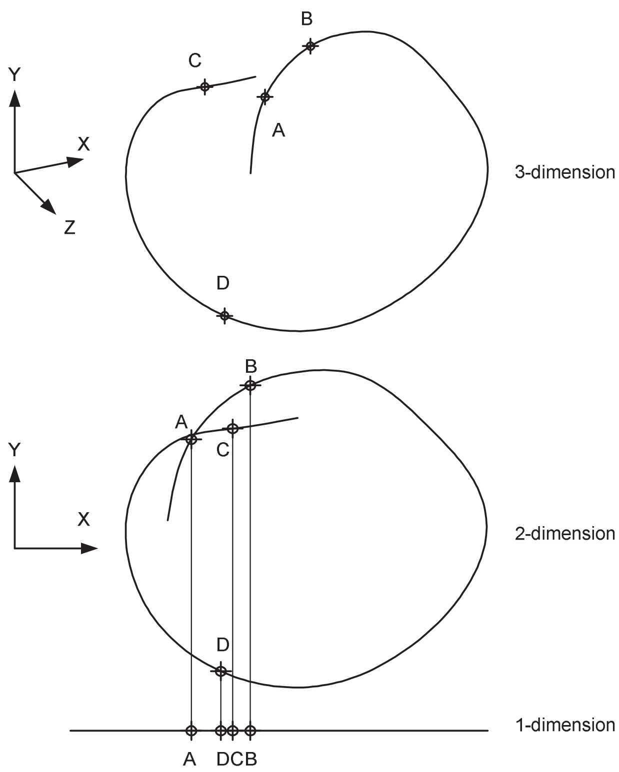

Fig. 1 An example of false nearest neighbors

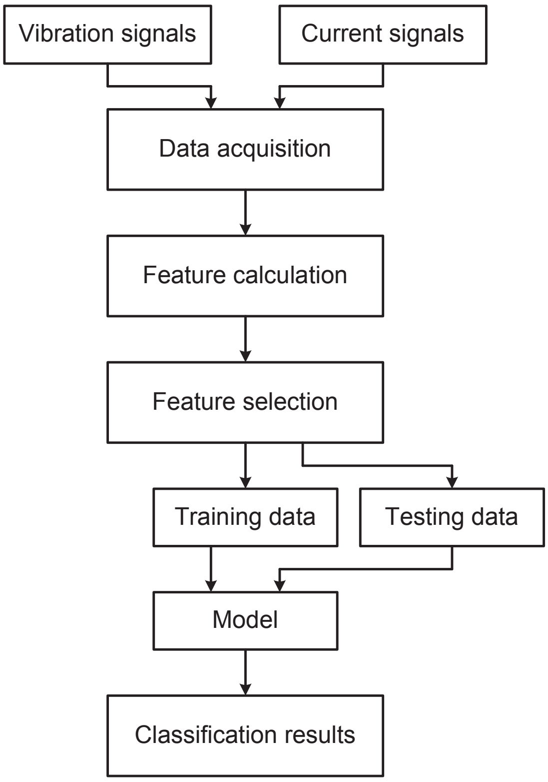

Fig. 2 Proposed system for fault diagnosis

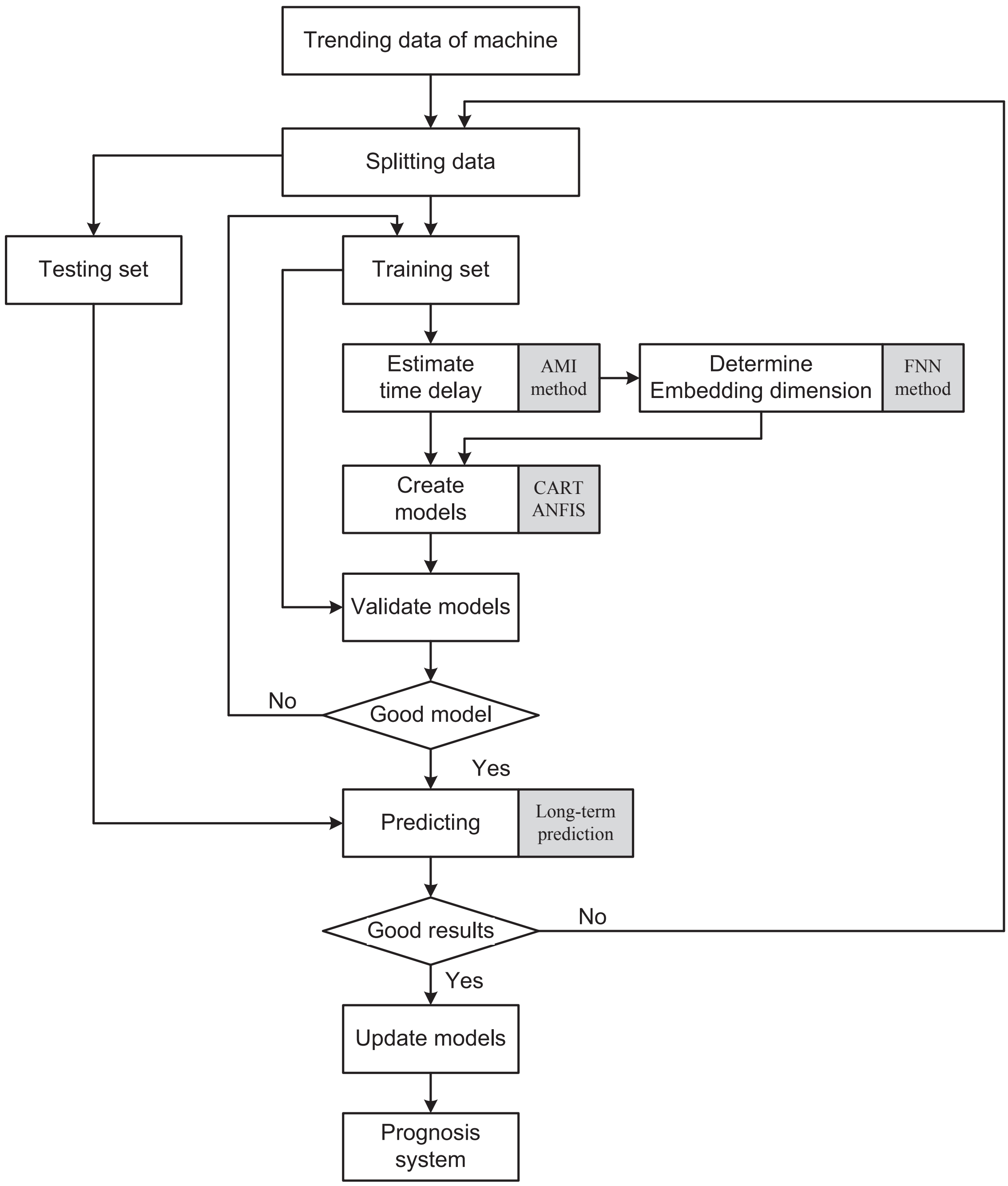

Fig. 3 Proposed system for machine condition prognosis

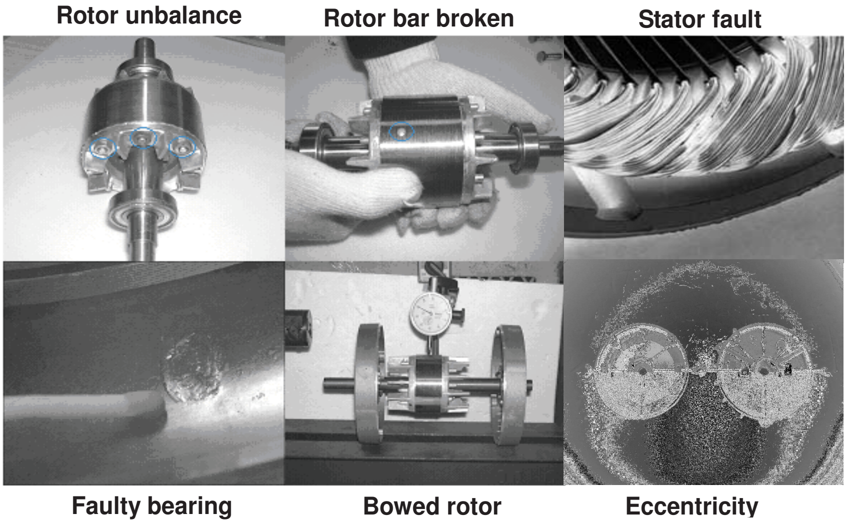

Fig. 4 Faults on the induction motors

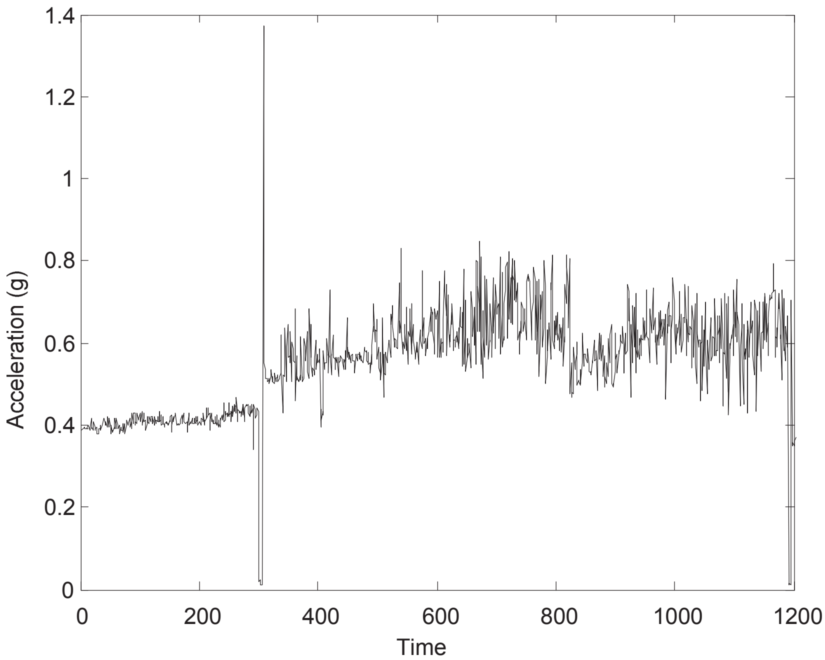

Fig. 5 The entire peak acceleration data of low methane compressor

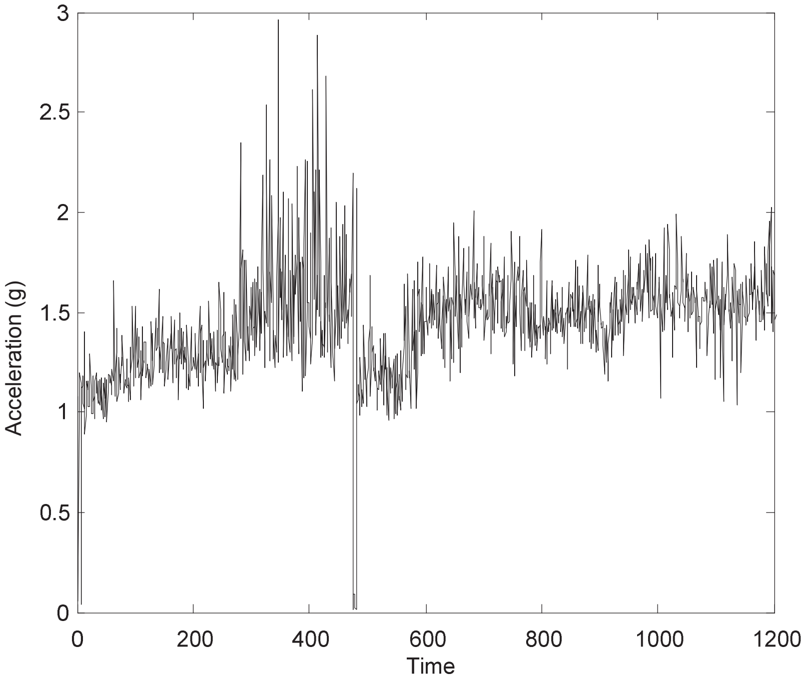

Fig. 6 The entire envelope acceleration data of low methane compressor

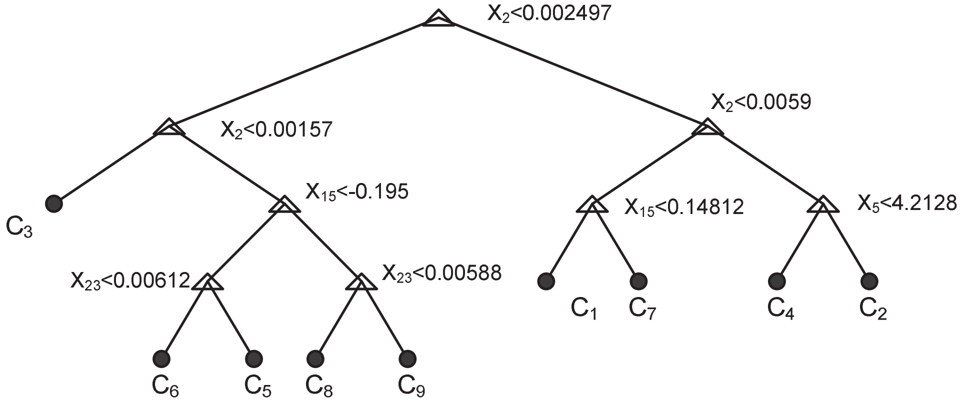

Fig. 7 Tree of features obtained from vibration signals

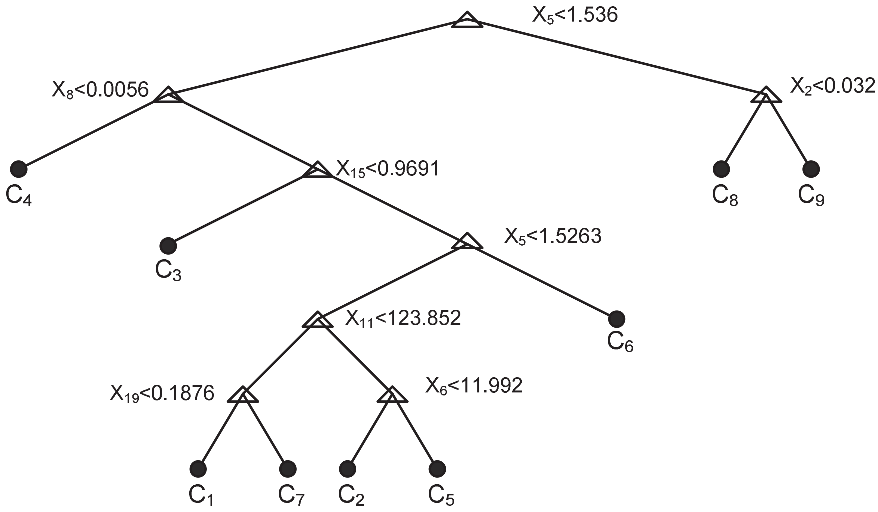

Fig. 8 Tree of features obtained from current signals

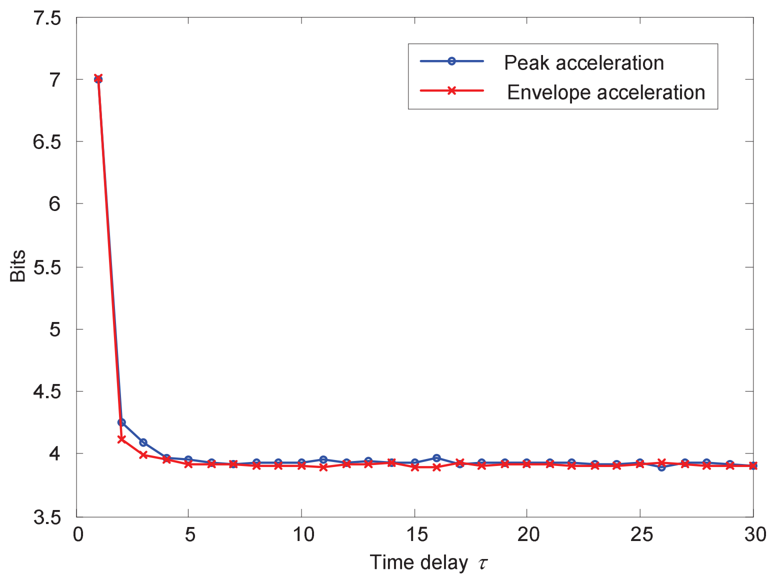

Fig. 9 Time delay estimation

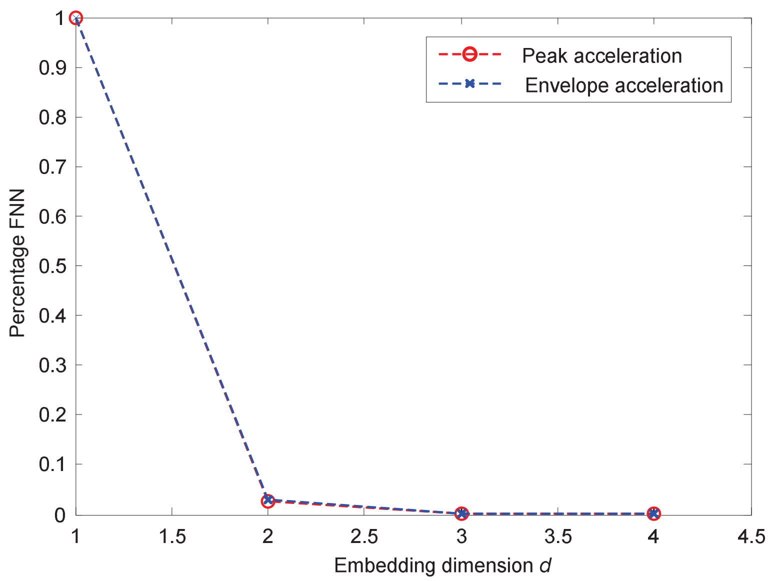

Fig. 10 The relationship between FNN percentage and embedding dimension

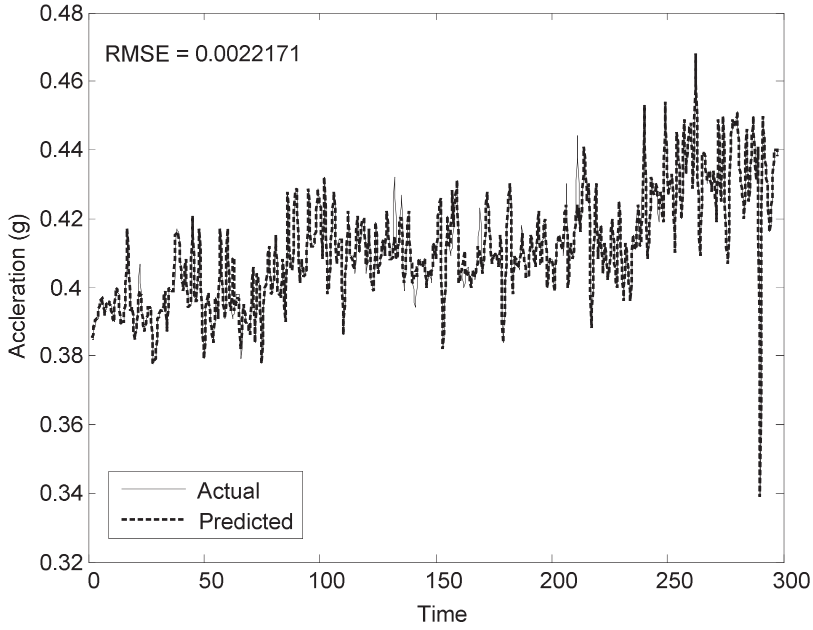

(a)

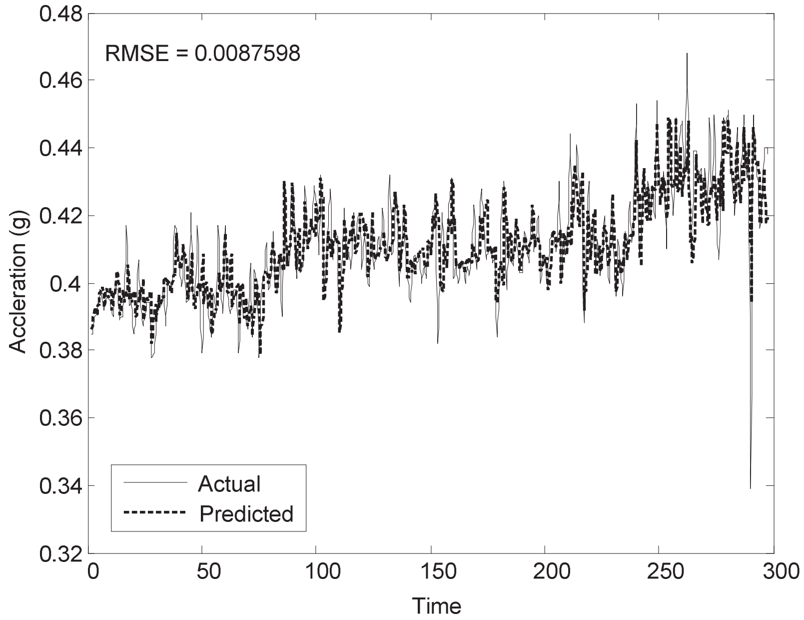

(b)

Fig. 11 Training and validating results of peak acceleration data. (a) CART, (b) ANFIS

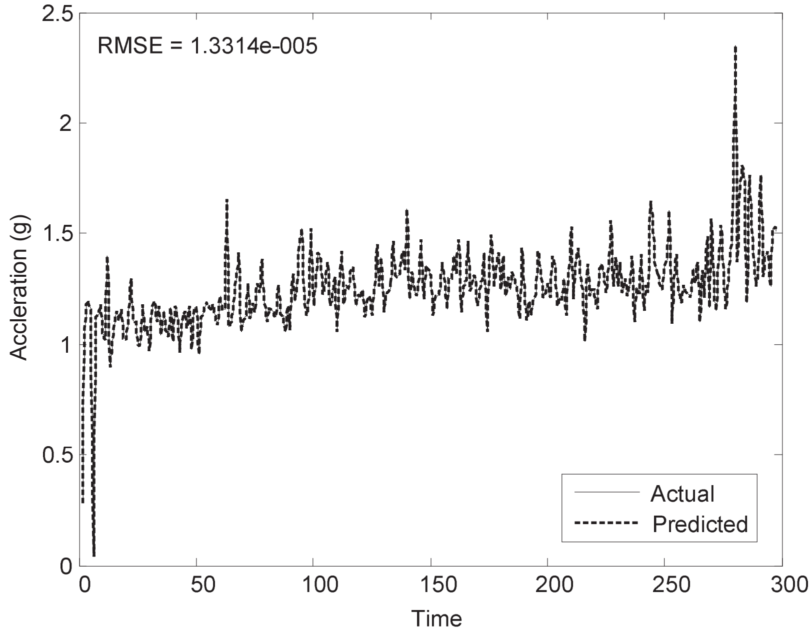

(a)

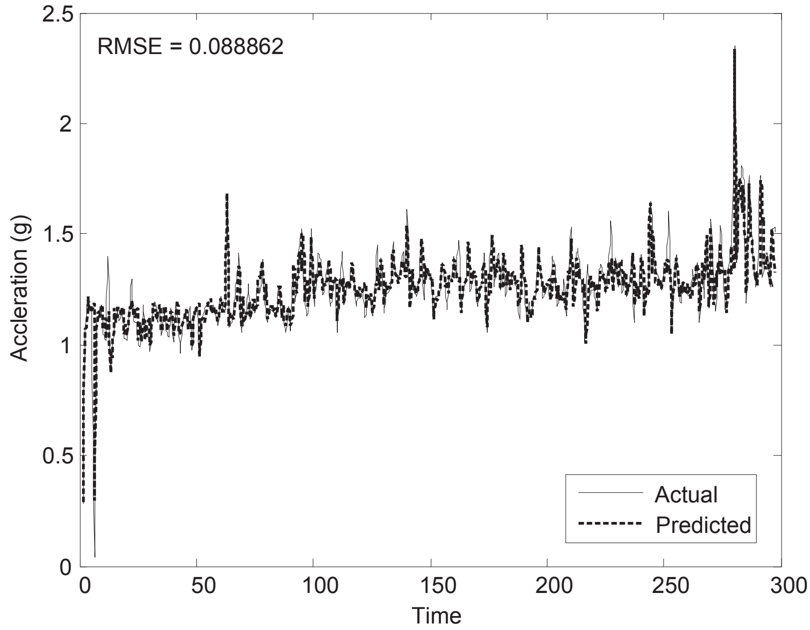

(b)

Fig. 12 Training and validating results of envelope acceleration data. (a) CART, (b) ANFIS

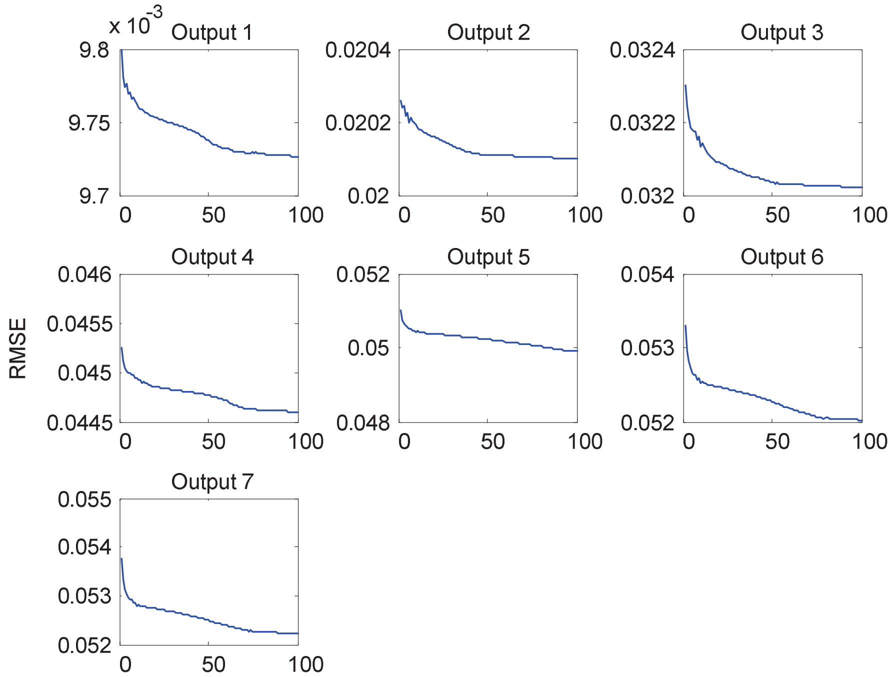

(a)

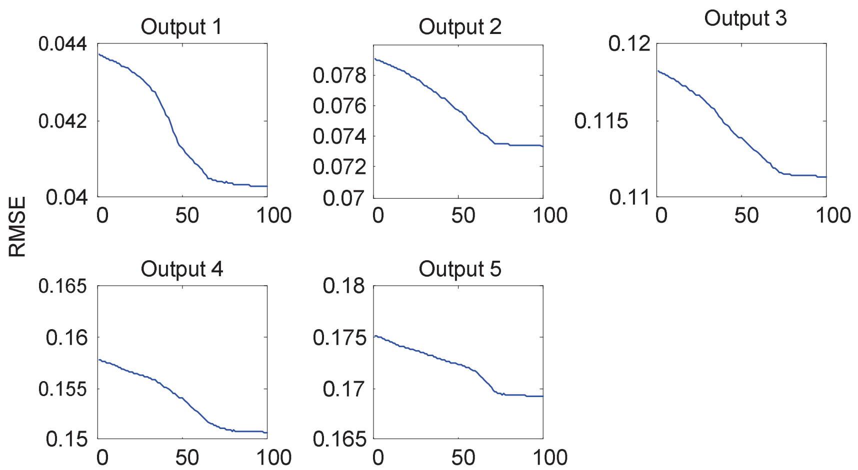

(b)

Fig. 13 RMSE convergent curve. (a) Peak acceleration, (b) Envelop acceleration

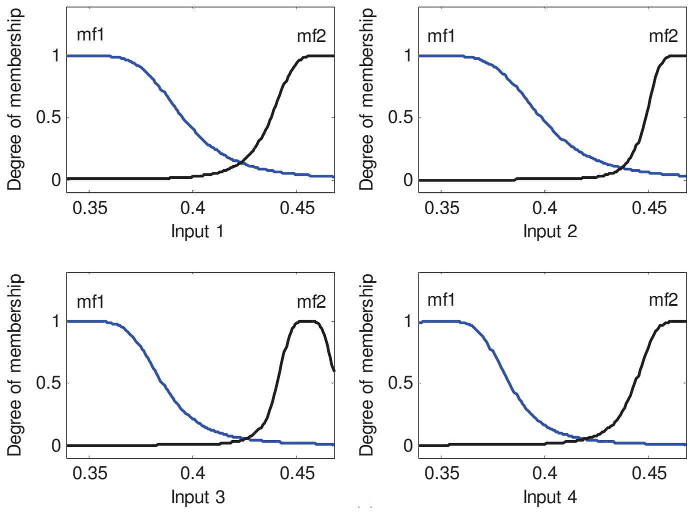

(a)

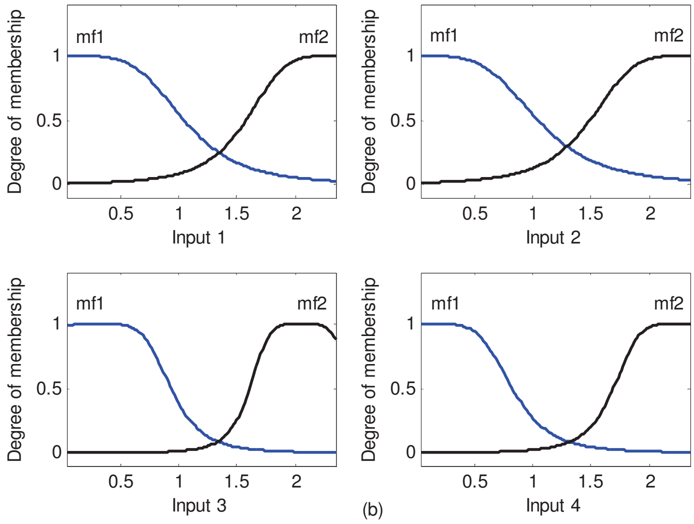

(b)

Fig. 14 The changes of MFs after learning. (a) Peak acceleration, (b) Envelop acceleration

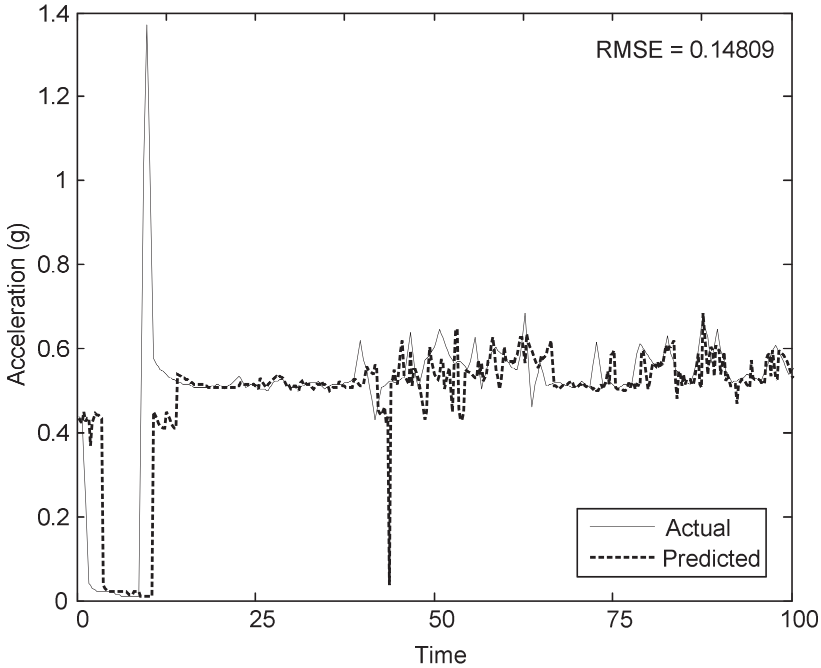

(a)

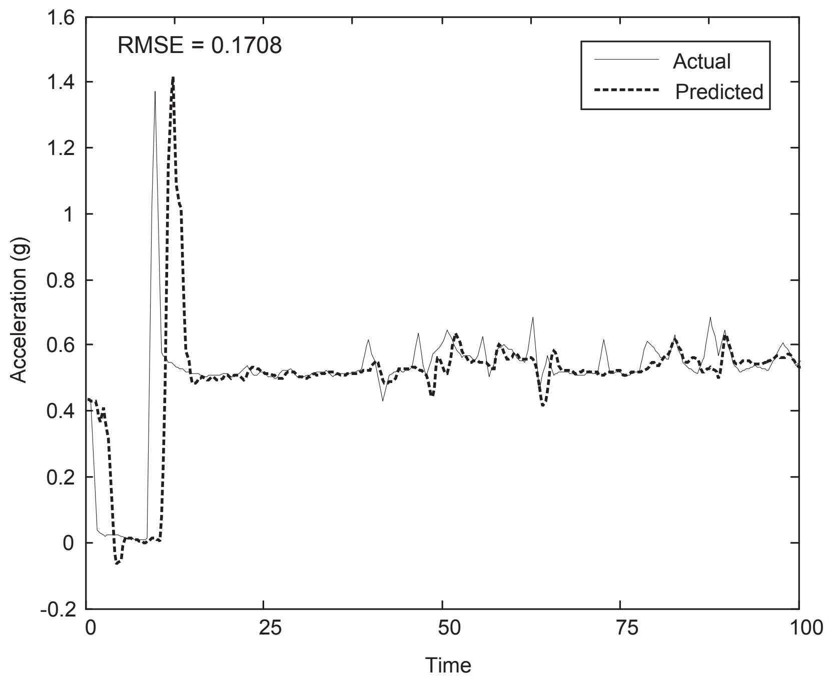

(b)

Fig. 15 Predicted results of peak acceleration data. (a) CART, (b) ANFIS.

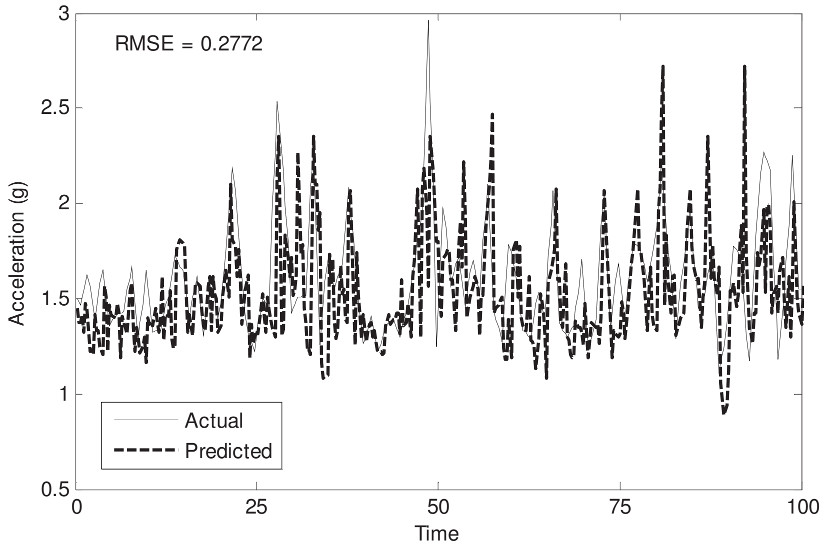

(a)

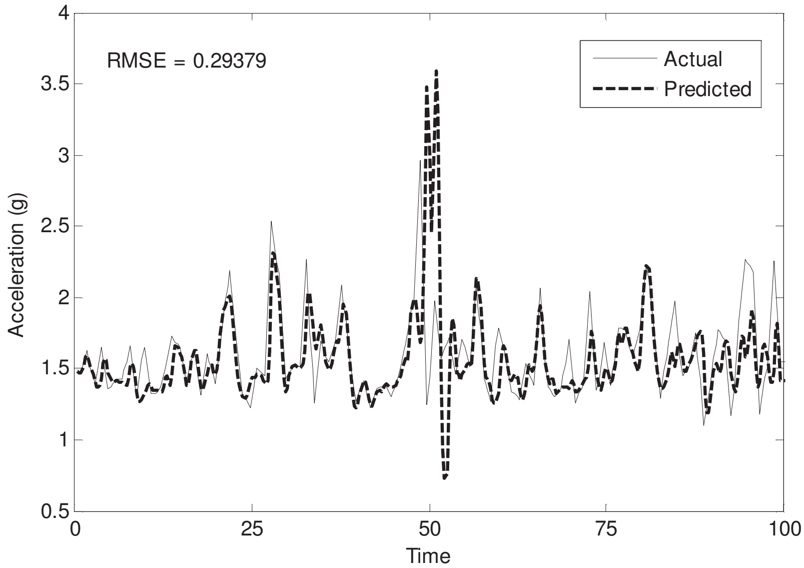

(b)

Fig. 16 Predicted results of envelop acceleration data. (a) CART, (b) ANFIS.

Table 1 The description of faulty motors

Fault condition	Fault description	Others
Broken rotor bar	Number of broken bar:12 ea	Total number of 34 bars
Bowed rotor	Max. shaft deflection: 0.075mm	Air-gap: 0.25mm
Faulty bearing	A spalling on outer raceway	#6203
Rotor unbalance	Unbalance mass on the rotor	8.4g
Eccentricity	Parallel and angular misalignments	Adjusting the bearing pedestal
Phase unbalance	Add resistance on one phase	8.4%

Table 2 Information of the system

Electric motor		Compressor	
Voltage	6600 V	Type	Wet screw
Power	440 kW	Lobe	Male rotor (4 lobes)
Pole	2 Pole		Female rotor (6 lobes)
Bearing	NDE:#6216, DE:#6216	Bearing	Thrust: 7321 BDB
RPM	3565 rpm		Radial: Sleeve type

Table 3 Feature parameters

Signals	Position	Feature parameters	
		Time domain	Frequency domain
Vibration	Vertical	Mean	RMS variance frequency
	Horizontal	RMS	Frequency center
	Axial	Shape factor	Root variance frequency
Current	Phase A	Skewness	
	Phase B	Kurtosis	
	Phase C	Crest factor	
		Entropy error	
		Entropy estimation	
		Histogram lower	
		Histogram upper	

Table 4 Descriptions of data sets

Label of classification	Condition	Number of training samples	Number of testing samples
C1	Angular misalignment	20	10
C2	Bowed rotor	20	10
C3	Broken rotor bar	20	10
C4	Bearing outer race fault	20	10
C5	Mechanical unbalance	20	10
C6	Normal condition	20	10
C7	Parallel misalignment	20	10
C8	Phase unbalance (30°)	20	10
C9	Phase unbalance (50°)	20	10
Total samples		180	90

Table 5 The confusion matrix for CART-ANFIS of 800 epochs

Output/ desired	Confusion matrix (vibration/current signals)								
	C1	C2	C3	C4	C5	C6	C7	C8	C9
C1	10/7	0/0	0/0	0/0	0/0	0/0	0/0	0/0	0/0
C2	0/0	10/8	0/0	1/0	1/0	0/0	1/1	0/1	0/0
C3	0/1	0/0	7/9	0/1	0/1	0/2	0/0	0/0	1/2
C4	0/0	0/0	0/0	9/8	0/1	0/0	0/1	0/1	0/0
C5	0/0	0/0	0/0	0/0	8/7	0/0	0/0	0/0	0/0
C6	0/0	0/0	0/0	0/0	0/0	10/7	0/0	0/0	0/0
C7	0/0	0/0	0/0	0/0	0/0	0/1	9/7	0/0	0/0
C8	0/2	0/2	1/1	0/1	1/0	0/0	0/0	10/8	0/0
C9	0/0	0/0	2/0	0/0	0/1	0/0	0/1	0/0	9/8

Table 6 The value of statistical parameters

Datasets label	Statistical parameters (vibration/current signals)		
	Sensitivity (%)	Specificity (%)	Total classification accuracy (%)
C1	100/70	100/100	91.11/76.67
C2	100/80	96.5/97.5	
C3	70/90	98.75/91.25	
C4	90/80	100/96.25	
C5	80/70	100/100	
C6	100/70	100/100	
C7	90/70	100/98.75	
C8	100/80	97.5/92.5	
C9	90/80	97.5/97.5	

Table 7 The RMSEs of CART and ANFIS

Data type	Training		Testing	
	CART	ANFIS	CART	ANFIS
Peak acceleration	0.002217	0.00876	0.14809	0.1708
Envelop acceleration	1.3314×10^{-5}	0.08886	0.2772	0.2938